Article
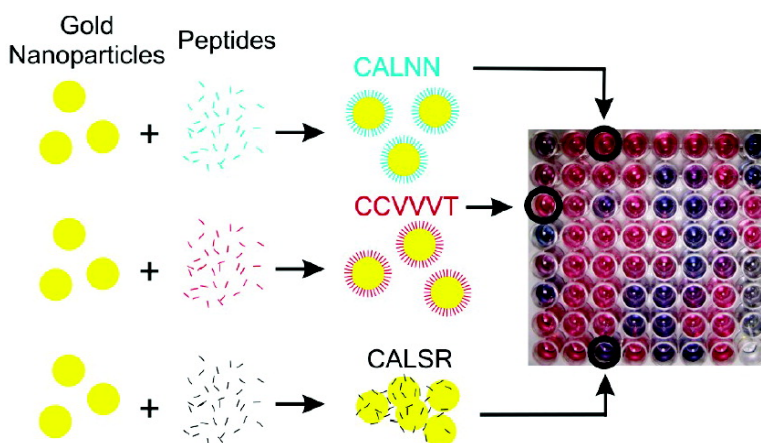
Rational and Combinatorial Design of Peptide Capping Ligands for Gold Nanoparticles

Raphal Lvy, Nguyen T. K. Thanh, R. Christopher Doty, Irshad Hussain,
Richard J. Nichols, David J. Schiffrin, Mathias Brust, and David G. Fernig

More About This Article

Additional resources and features associated with this article are available within the HTML version:

- Supporting Information
- Links to the 24 articles that cite this article, as of the time of this article download
- Access to high resolution figures
- Links to articles and content related to this article
- Copyright permission to reproduce figures and/or text from this article

View the Full Text HTML

Rational and Combinatorial Design of Peptide Capping Ligands for Gold Nanoparticles

Raphaël Lévy,*[†,‡,§] Nguyen T. K. Thanh,[†,‡,§] R. Christopher Doty,[†,‡,§]
Irshad Hussain,[†,§] Richard J. Nichols,[†,§] David J. Schiffrin,[†,§] Mathias Brust,[†,§] and
David G. Fernig[†,‡]

*Contribution from the Center for Nanoscale Science, School of Biological Sciences,
Bioscience Building, and Department of Chemistry, University of Liverpool,
Liverpool L69 7ZB, U.K.*

Received March 5, 2004; E-mail: rapha@liverpool.ac.uk; dgfernig@liverpool.ac.uk

Abstract: Based on protein folding considerations, a pentapeptide ligand, CALNN, which converts citrate-stabilized gold nanoparticles into extremely stable, water-soluble gold nanoparticles with some chemical properties analogous to those of proteins, has been designed. These peptide-capped gold nanoparticles can be freeze-dried and stored as powders that can be subsequently redissolved to yield stable aqueous dispersions. Filtration, size-exclusion chromatography, ion-exchange chromatography, electrophoresis, and centrifugation can be applied to these particles. The effect of 58 different peptide sequences on the electrolyte-induced aggregation of the nanoparticles was studied. The stabilities conferred by these peptide ligands depended on their length, hydrophobicity, and charge and in some cases resulted in further improved stability compared with CALNN, yielding detailed design criteria for peptide capping ligands. A simple strategy for the introduction of recognition groups is proposed and demonstrated with biotin and Strep-tag II.

Introduction

Since their development 10 years ago[1] thiol-capped gold nanoparticles have been extensively studied covering a broad range of structural, electronic, optical, and chemical aspects.[2-7] A prerequisite for most of these studies and thus an extremely important feature of these particles is their superb stability at ambient conditions resulting from the very effective surface passivation by the thiol capping agent. Most research to date has focused on nonpolar, alkanethiol-capped particles of 1–4 nm diameter, which are insoluble in water. These are usually referred to as monolayer protected clusters (MPCs). Their unique properties have been widely established only for materials of this composition and size range. Considering the broad range of technological applications that are envisaged for MPCs, those related to bioanalytical and biomedical problems appear to be the most promising at present.[8-16] These, however, require high

stability and solubility in aqueous media combined with a controllable chemical reactivity of the ligand shell and preferably, high optical detectability down to the individual particle level. While a number of promising preparative approaches to stable, water-soluble MPCs have been developed, few of these, if any, lead to materials that are comparable to the well-described nonpolar species in terms of stability and chemical versatility. Previously reported strategies include the use of thiol ligands with hydrophilic end groups such as poly(ethylene glycol),[17-21] silica encapsulation of the metal cluster,[22,23] polymeric capping agents such as amino- or mercaptodextrans,[24] and BSA.[25,26] Probably the most widely studied systems are the tiopronin-
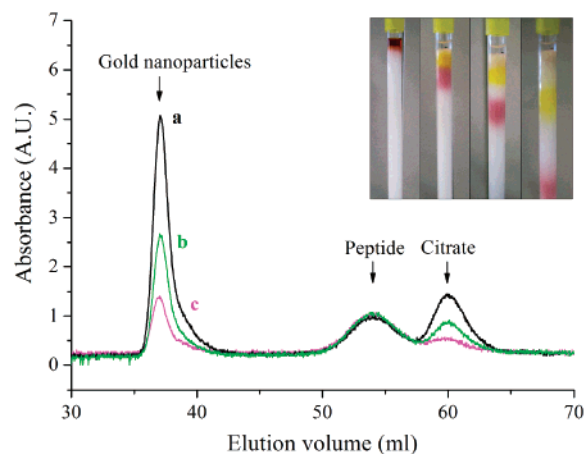
---

† Center for Nanoscale Science.
‡ School of Biological Sciences.
§ Department of Chemistry.

(1) Brust, M.; Walker, M.; Bethell, D.; Schiffrin, D. J.; Whyman, R. *J. Chem. Soc., Chem. Commun.* **1994**, 801–802.
(2) Hostetler, M. J.; Murray, R. W. *Curr. Opin. Colloid Interface Sci.* **1997**, *2*, 42–50.
(3) Templeton, A. C.; Wuelfing, M. P.; Murray, R. W. *Acc. Chem. Res.* **2000**, *33*, 27–36.
(4) Whetten, R. L.; Shafigullin, M. N.; Khoury, J. T.; Schaaff, T. G.; Vezmar, I.; Alvarez, M. M.; Wilkinson, A. *Acc. Chem. Res.* **1999**, *32*, 397–406.
(5) Brust, M.; Kiely, C. J. *Colloids Surf.* **2002**, *202*, 175–186.
(6) Brust, M.; Kiely, C. J. In *Colloids and colloid assemblies*; Caruso, F., Ed.; Wiley-VCH: Weinheim, 2004; pp 96–119.
(7) Daniel, M. C.; Astruc, D. *Chem. Rev.* **2004**, *104*, 293–346.
(8) Yguerabide, J.; Yguerabide, E. E. *Anal. Biochem.* **1998**, *262*, 137–156.
(9) Yguerabide, J.; Yguerabide, E. E. *J. Cell. Biochem.* **2001**, *84*, 71–81.
(10) Yguerabide, J.; Yguerabide, E. E. *Anal. Biochem.* **1998**, *262*, 157–176.
(11) Schultz, D. A. *Curr. Opin. Biotechnol.* **2003**, *14*, 13–22.
(12) Schultz, S.; Smith, D. R.; Mock, J. J.; Schultz, D. A. *Proc. Natl. Acad. Sci. U. S. A.* **2000**, *97*, 996–1001.
(13) Taton, T. A.; Mirkin, C. A.; Letsinger, R. L. *Science* **2000**, *289*, 1757–1760.
(14) Kanaras, A. G.; Wang, Z. X.; Bates, A. D.; Cosstick, R.; Brust, M. *Angew. Chem., Int. Ed.* **2003**, *42*, 191–194.
(15) *Nanobiotechnology: Concepts, Applications and Perspective*; Niemeyer, C. M., Mirkin, C. A., Eds.; Wiley-VCH: Weinheim, 2004.
(16) Alivisatos, P. *Nat. Biotechnol.* **2004**, *22*, 47–52.
(17) Wuelfing, W. P.; Gross, S. M.; Miles, D. T.; Murray, R. W. *J. Am. Chem. Soc.* **1998**, *120*, 12696–12697.
(18) Bartz, M.; Kuther, J.; Nelles, G.; Weber, N.; Seshadri, R.; Tremel, W. *J. Mater. Chem.* **1999**, *9*, 1121–1125.
(19) Foos, E. E.; Snow, A. W.; Twigg, M. E.; Ancona, M. G. *Chem. Mater.* **2002**, *14*, 2401–2408.
(20) Kanaras, A. G.; Kamounah, F. S.; Schaumburg, K.; Kiely, C. J.; Brust, M. *Chem. Commun.* **2002**, 2294–2295.
(21) Pengo, P.; Polizzi, S.; Battagliarin, M.; Pasquato, L.; Scrimin, P. *J. Mater. Chem.* **2003**, *13*, 2471–2478.
(22) Mulvaney, P.; Liz-Marzan, L. M.; Giersig, M.; Ung, T. *J. Mater. Chem.* **2000**, *10*, 1259–1270.
(23) Mulvaney, S. P.; Musick, M. D.; Keating, C. D.; Natan, M. J. *Langmuir* **2003**, *19*, 4784–4790.
(24) Wilson, R. *Chem. Commun.* **2003**, 108–109.
(25) Tkachenko, A. G.; Xie, H.; Coleman, D.; Glomm, W.; Ryan, J.; Anderson, M. F.; Franzen, S.; Feldheim, D. L. *J. Am. Chem. Soc.* **2003**, *125*, 4700–4701.

capped gold nanoparticles developed by Murray et al.[27] Although stability problems have in some cases been successfully addressed, a remaining general shortcoming of most preparative methods is the lack of generic protocols for the functionalization of particles with biomolecules. The present work demonstrates a general approach to the synthesis of extremely stable gold nanoparticles that are readily biofunctionalized by standard techniques.

Within living systems the generic, nonaggregating nanoparticles par excellence are proteins. It should be noted, however, that only a relatively small subset of all possible polypeptides does not flocculate under physiological conditions. Naturally occurring, water-soluble proteins obviously belong to this nonaggregating subset. In light of this comment, it is not surprising that gold nanoparticles often aggregate from aqueous solution when thiol-containing amino acids or peptides are added as capping agents.[28] Nonaggregating proteins are usually able to fold in such a way that their hydrophobic groups are located in the interior part of the macromolecule, while charged and hydrophilic groups are exposed to water. It is also important to be able to avoid electrostatic aggregation, caused by attractive interactions between ammonium and carboxylate moieties. This is best achieved by ensuring that the particles have a positive or negative net charge, leading to overall repulsive interactions.

Based on these considerations, a pentapeptide thiol capping ligand that converts citrate-stabilized gold nanoparticles into stable, water-soluble MPCs with chemical properties comparable to those of proteins has been designed. The basic design principle was to create a ligand that would readily attach to the surface of the gold particle and form a well-packed passivating layer with a hydrophilic terminus. A combinatorial approach was then used to test variations of this theme and demonstrate that the design rationale was indeed reasonable. The stability of the various particle preparations has been evaluated by exposing the particles to increasing sodium chloride concentrations until precipitation occurred. Extremely stable, water-soluble gold nanoparticles have been obtained in this way, and basic design criteria could be established by comparing the relative stabilities conferred to the particles by different peptide ligands. Moreover, a peptide that provides increased stability over the originally designed peptide has been identified.

Results and Discussion

Rational Design of the Pentapeptide Initially Used. The design strategy of the peptide initially studied took into account the need to have a strong affinity for gold, ability to self-assemble into a dense layer that excludes water, and a hydrophilic terminus, which would ensure solubility and stability in water. The pentapeptide CALNN (Chart 1) was designed to achieve these goals. The thiol group in the side chain of the N-terminal cysteine (C) is able to make a covalent bond to the gold surface. This interaction may be additive to that of the N-terminal primary amine, since amino groups are also known to have a strong interaction with gold surfaces.[29] Moreover, it has been shown by Gordillo and co-workers that the presence

Figure 1. Rapid stabilization of gold nanoparticles by CALNN. Spectra of citrate and peptide-capped gold nanoparticles after mixing with (a) one volume of water, (b) one volume of 1.38 mM CALNN in phosphate-buffered saline, and (c) one volume of phosphate-buffered saline.

Chart 1. CALNN Structure

of a positively charged ammonium group in the vicinity of the thiol significantly accelerates the adsorption kinetics of thiols onto citrate-stabilized gold nanoparticles.[30] Alanine (A) and leucine (L) in positions 2 and 3 possess hydrophobic side chains and were chosen to promote the self-assembly of the peptide. The leucine side chain is larger than that of alanine to take into account the curvature of the nanoparticle. Asparagine (N) in positions 4 and 5 is an uncharged, but hydrophilic amino acid due to the amide group on the side chain, and the C-terminal asparagine in position 5 can bear a negative charge due to the terminal carboxylic group.

Rapid Stabilization of Citrate Gold Nanoparticles. Citrate gold nanoparticles are stable in water and display a characteristic UV−vis absorption spectrum with a plasmon band at 520 nm (Figure 1a).

The absorption spectrum is sensitive to the nanoparticle environment, and this has been used to design different bioassays.[31−33] On addition of sodium chloride, citrate nanoparticles aggregate due to the screening of the electrostatic repulsion between them, and consequently the absorption spectrum is significantly modified with a decrease of the plasmon band at 520 nm and an increased absorbance at longer wavelengths (Figure 1c).[30] When CALNN is added together with sodium chloride, the plasmon band absorbance increases slightly and a 2 nm shift of the maximum is observed (Figure 1b). The shift occurs in a few seconds, and the spectrum is then stable

(26) Xie, H.; Tkachenko, A. G.; Glomm, W. R.; Ryan, J. A.; Brennaman, M. K.; Papanikolas, J. M.; Franzen, S.; Feldheim, D. L. *Anal. Chem.* **2003**, *75*, 5797−5805.

(27) Templeton, A. C.; Chen, S. W.; Gross, S. M.; Murray, R. W. *Langmuir* **1999**, *15*, 66−76.

(28) Pengo, P.; Broxterman, Q. B.; Kaptein, B.; Pasquato, L.; Scrimin, P. *Langmuir* **2003**, *19*, 2521−2524.

(29) Zhang, J.; Chi, Q.; Nielsen, J. U.; Friis, E. P.; Andersen, J. E. T.; Ulstrup, J. *Langmuir* **2000**, *16*, 7229−7237.

(30) Bellino, M. G.; Calvo, E. J.; Gordillo, G. *Phys. Chem. Chem. Phys.* **2004**, *6*, 424−428.

(31) Nath, N.; Chilkoti, A. *Anal. Chem.* **2002**, *74*, 504−509.

(32) Riboh, J. C.; Haes, A. J.; McFarland, A. D.; Yonzon, C. R.; Van Duyne, R. P. *J. Phys. Chem. B* **2003**, *107*, 1772−1780.

(33) Englebienne, P.; Van Hoonacker, A.; Verhas, M. *Analyst* **2001**, *126*, 1645−1651.

Figure 2. Size-exclusion chromatography of CALNN-capped nano-particles. Chromatographs of three samples with (a) 14.1, (b) 7.0, and (c) 3.5 nM gold nanoparticles obtained by dilution in water and a constant concentration of peptide. Inset: pictures showing the separation of potassium dichromate (yellow) and CALNN-capped gold nanoparticles (red). Potassium dichromate and gold nanoparticles were mixed just prior to loading on the column.

for weeks. This is due to the local change of dielectric permittivity, resulting from the formation of a peptide layer on the surface of the nanoparticles. Thus, the peptide provides immediate protection to the particles from the electrolyte-induced aggregation. The rapid protection reaction may be driven by an initial uptake of the peptide via electrostatic interaction (positively charged amino group toward the negatively charged gold surface),[30] which directs the thiol onto the Au surface. Nevertheless, it seems that a very small improvement of particle stability is still obtained after 24 h incubation (data not shown). In what follows, the size-exclusion chromatography, ion-exchange chromatography, and handling properties of the CALNN-capped nanoparticles will be discussed.

Purifying and Handling CALNN-Capped Nanoparticles. Centrifugation can be used for the separation of CALNN-capped gold nanoparticles, as previously observed for DNA or polymer stabilized particles. CALNN-capped gold nanoparticles can be freeze-dried and stored as a powder for further utilization, and when redissolved in water, they display exactly the same UV−vis absorption spectrum as before freeze-drying (Supporting Information). This is an important result, since very few preparations can be stored in the dry state and then redispersed in water.[34] CALNN-capped gold nanoparticles can also be sterilized by filtration through a 0.22 μm filter without any detectable loss of material (Supporting Information), which is extremely useful for biological applications. Perhaps the most useful property is that CALNN-capped nanoparticles are compatible with standard liquid chromatography media used in protein purification. Similarly to a protein, this allows purification based on affinity tags, size, or charge.

Size-exclusion chromatography on Sephadex G25 provides a rapid means to separate the peptide-capped gold nanoparticles from the excess peptide and citrate (Figure 2). The first peak corresponds to the void volume of the column and contains the functionalized gold nanoparticles. The second and third peaks correspond, respectively, to the free peptide and to the free

citrate ions. As expected, the amplitude of the citrate peak scales with the nanoparticle concentration. Attribution of the peaks has been confirmed by control experiments with peptide and citrate alone and by UV−vis spectroscopy. The ability of the technique for the separation of gold nanoparticles from reagents is illustrated by the separation of potassium dichromate (yellow) from the red solution of nanoparticles (Figure 2, inset). The advantage of separation by size-exclusion chromatography over centrifugation is that it is possible to change in a single gentle but quick step the medium surrounding the particles, thus allowing multistep reactions. In addition, the process can be easily scaled up for preparative and production purposes. Chromatography of aqueous solutions of nanoparticles has, in many cases, been hampered by adsorption of the particles on the high surface of the stationary phase. This problem has been solved by using surfactants[35] or other stabilizers in the eluent.[36] Size-exclusion chromatography provides also a means to measure the size distribution of the particles and to purify them as a function of their size. This has been recently demonstrated for gold and silver particles dispersed in organic solvents.[37,38]

The peptide-capped nanoparticles could also be separated in an anion-exchange column. The particles were first bound to the gel at low ionic strength and then eluted by increasing the ionic strength (Supporting Information). This provides a means of purifying gold nanoparticles as a function of their charge. In the present case, it also demonstrates that the particles are negatively charged and hence that the peptides are oriented with the carboxylic group directed toward the solvent.

In addition, the peptide-capped nanoparticles were characterized by gel electrophoresis. Their electrophoretic mobility in a 1% agarose gel was found to be similar to that of a 600 base pair DNA (Supporting Information).

Stability of Peptide-Capped Gold Nanoparticles in Aqueous Buffer. To be useful for biological applications or for building nanostructures using biological interactions, gold nanoparticles have to be stable over a wide range of ionic strength and pH in the absence of an excess of capping ligand. CALNN-capped nanoparticles were first separated from the excess of peptide and citrate by size-exclusion chromatography. Figure 3A shows that the CALNN-capped nanoparticles are stable up to a NaCl concentration of 1 M at pH 7, with no detectable change in the UV−vis absorbance spectrum. NaCl-induced aggregation occurs at 1.25 M NaCl and is more pronounced at 1.5 M, as can be seen from the decrease of the absorbance at 522 nm and the increase in absorbance at longer wavelengths. The aggregation of gold nanoparticles leads to a new absorption band at longer wavelengths due to dipole coupling between the plasmons of neighboring particles forming the aggregates.[39,40] As an empirical measurement of the aggregation process, an aggregation parameter, which measures the variation of the integrated absorbance between 600 and 700 nm, was used. The aggregation parameter AP is defined as follows: $\text{AP} = (A - A_0)/A_0$, where A is the integrated

(34) Mangeney, C.; Ferrage, F.; Aujard, I.; Marchi-Artzner, V.; Jullien, L.; Ouari, O.; Rekai, E. D.; Laschewsky, A.; Vikholm, I.; Sadowski, J. W. *J. Am. Chem. Soc.* **2002**, *124*, 5811−5821.

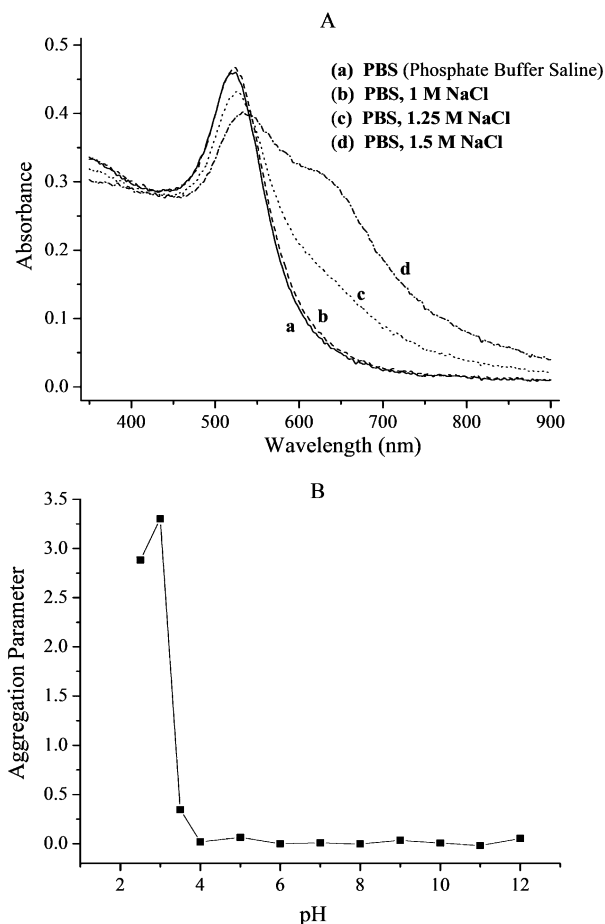(35) Wei, G. T.; Liu, F. K. *J. Chromatogr., A* **1999**, *836*, 253−260.
(36) Siebrands, T.; Giersig, M.; Mulvaney, P.; Fischer, C. H. *Langmuir* **1993**, *9*, 2297−2300.
(37) Wilcoxon, J. P.; Martin, J. E.; Provencio, P. *J. Chem. Phys.* **2001**, *115*, 998−1008.
(38) Wilcoxon, J. P.; Martin, J. E.; Provencio, P. *Langmuir* **2000**, *16*, 9912−9920.
(39) Kreibig, U.; Genzel, L. *Surf. Sci.* **1985**, *156*, 678−700.
(40) Storhoff, J. J.; Lazarides, A. A.; Mucic, R. C.; Mirkin, C. A.; Letsinger, R. L.; Schatz, G. C. *J. Am. Chem. Soc.* **2000**, *122*, 4640−4650.

A

(a) **PBS** (Phosphate Buffer Saline)
(b) **PBS, 1 M NaCl**
(c) **PBS, 1.25 M NaCl**
(d) **PBS, 1.5 M NaCl**

B

Figure 3. UV−vis study of CALNN-capped nanoparticle stability as a function of (A) NaCl concentration at pH 7 (phosphate-buffered solution) and (B) pH.

absorbance between 600 and 700 nm of the sample at a given moment and A_0 is the integrated absorbance between 600 and 700 nm of the initial, fully dispersed solution of nanoparticles. A similar indicator has been used to analyze the aggregation of gold and silver particles induced by the biotin−avidin interaction[41,42] and to study the interfacial phase transition of a thermally responsive biopolymer adsorbed onto gold nanoparticles.[43]

CALNN-capped nanoparticles are stable at basic, neutral, and slightly acidic pH. However, below pH 4 they start to aggregate, as evidenced by the change in the aggregation parameter (Figure 3B). This is expected, since the terminal carboxylic group pK_a is 4,[44] so electrostatic repulsion between particles is reduced. This aggregation is reversible, and adding NaOH to the solution allows a complete recovery of the initial spectrum.

Combinatorial Design. CALNN is one of 3 200 000 possible sequences of five natural amino acids. Its sequence was chosen from existing knowledge of protein structure and amino acid side chain packing/bonding properties. The remarkable stability that CALNN imparts to gold nanoparticles raised several questions. Is it the predicted interactions of CALNN amino acid side chains that provide such stability? What are the properties

(41) Sastry, M.; Lala, N.; Patil, V.; Chavan, S. P.; Chittiboyina, A. G. *Langmuir* **1998**, *14*, 4138−4142.
(42) Weisbecker, C. S.; Merritt, M. V.; Whitesides, G. M. *Langmuir* **1996**, *12*, 3763.
(43) Nath, N.; Chilkoti, A. *J. Am. Chem. Soc.* **2001**, *123*, 8197−8202.
(44) Tandford, C. *Adv. Protein Chem.* **1962**, *17*, 69−165.

of peptides required to obtain this stability, and would other sequences lead to similar or better stability for gold nanoparticles?

These issues were further investigated by studying the effect of systematic variations of the peptide sequence on stability. All sequences tested are listed in Table 1. The variation criteria were the peptide length, the anchor (first amino acid), the peptide core (second and third amino acids), and the peptide carboxy terminus (fourth and fifth amino acids). Nine sequences with no direct relation to CALNN were also tried to test new designs (Table 1). These were based on hydrogen bonding and β-strand formation, and the presence of the thiol (cysteine) in the middle or at both ends of the peptide. The effect of these 58 peptides on the electrolyte-induced aggregation of gold nanoparticles was studied. Since some of the peptides are very hydrophobic, dimethyl sulfoxide (DMSO) was used as the common solvent for the 58 peptides for their incorporation in the aqueous gold colloid solution, to facilitate the comparison of the sequences. After 1 h the pH was adjusted to 7 and the NaCl concentration progressively increased while the absorbance spectra were monitored.

Figures 4−7 show the aggregation parameter as a function of NaCl concentration for different series of peptides. Due to the large volume of data, the spectra are represented by the aggregation parameter previously defined; complete spectra are presented in the Supporting Information.

Peptides Inducing Aggregation. For 19 of the investigated sequences (Table 1), the addition of peptide induced an immediate aggregation of the particles. These peptides share the ability of bridging two particles together as a common structural feature. Most of them bear an amino (on the lysine, K) or guanidino (on the arginine, R) group distal to the thiol. These groups have a strong affinity for gold. NNLAC, the reverse sequence of CALNN, induces aggregation for the same reason. Apart from directionality, the only difference between these two peptides is that in CALNN the amino terminal group is on the cysteine bearing the thiol group, but on NNLAC the cysteine's thiol is adjacent to the terminal carboxylic acid and the amino terminal group is on the asparagine (N) in position 1. CAALPDGLAAC and CVVITPDGTIVVC also induce aggregation, probably due to the presence of the two terminal thiols, which may bridge nanoparticles. It might still be possible to prepare stable particles with some of these sequences by varying buffers, particle concentrations, and order of mixing.[45] More investigations on this peptide-induced aggregation are underway. The amino acid sequences that promote aggregation will not be discussed further.

Influence of the First Amino Acid (Anchorage) and of Peptide Length. Figure 4A shows the effect of peptide length on nanoparticle stability. For a two amino acid peptide (CA), the aggregation parameter increases rapidly with NaCl concentration. As the length of the peptide increases from CA to CAL, CALN, and finally to CALNN, the NaCl-induced aggregation is displaced to increasingly higher concentrations of NaCl, suggestive of a direct correlation between peptide length and stability of the peptide-capped nanoparticles (Figure 4A). The apparent contradiction between Figure 3A, where CALNN-capped nanoparticles are shown to be stable at a concentration

(45) Shipway, A. N.; Lahav, M.; Gabai, R.; Willner, I. *Langmuir* **2000**, *16*, 8789−8795.

Table 1. List of Peptide Sequences Tested as Capping Ligands[a]

length	anchor substitution in position 1, and reverse sequence of CALNN	core hydrophobic residues substituted in positions 2 and 3	core hydrophilic residues substituted in positions 2 and 3	terminal substitution in positions 4 and 5	new design
CA	KALNN	CILNN	CKLNN	CALLS	CTTTT
CAL	AALNN	CLLNN	CDLNN	CALLD	CHRIS[b]
CALN	CALNN	CVLNN	CTLNN	CALLK[b]	CVVIT
CALNN	CCALNN	CFLNN	CNLNN	CALLR[b]	CCVVVT
	NNLAC[b]	CAANN	CAKNN[b]	CALNS	CCVVVK[b]
	NNLAC[b,c]	CAINN	CADNN	CALND	CAALPDGLAAC[b,c]
		CAVNN	CATNN	CALNK[b]	CVVITPDGTIVVC[b]
		CAFNN	CANNN	CALNR[b]	NNLACALNN
		CLANN	CDDNN	CALSS	NNLACCALNN
			CKKNN[b]	CALSD	
			CTTNN	CALSK[b]	
			CTSNN	CALSR[b]	
				CALKS[b]	
				CALKD	
				CALKK[b]	
				CALLS[b,c]	
				CALSS[b,c]	
				CALKK[b,c]	
				CALNN[b,c]	

[a] The sequences shown in each column have been modified according to the variation criteria of the column headings. [b] Peptide addition induced immediate nanoparticle aggregation. These sequences were ignored in the sodium chloride induced aggregation analysis (Figures 4-7). [c] C-terminal amide.
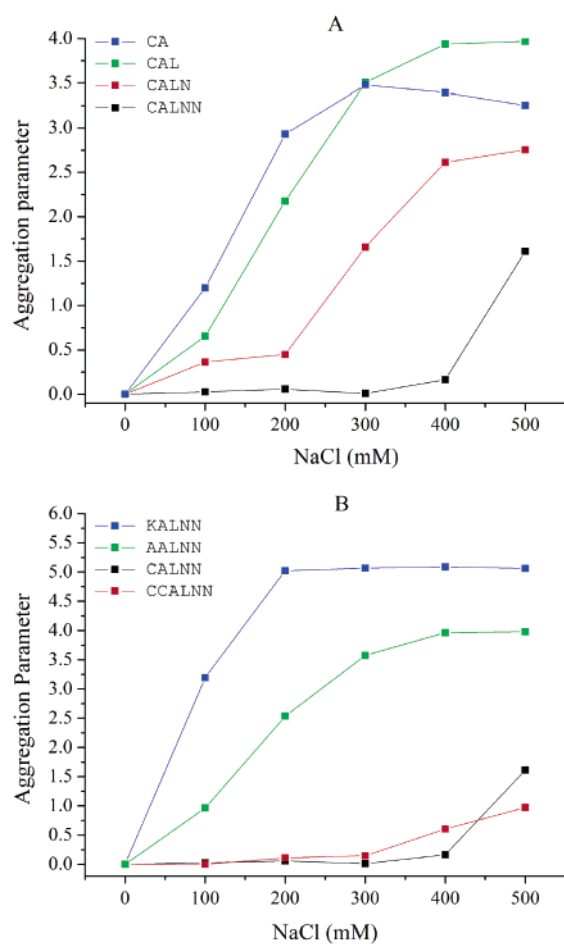
Figure 4. Effect of peptide length (A) and anchorage chemistry (B) on stability of gold nanoparticles.

of 1 M NaCl, and the aggregation at 500 mM in Figure 4A is probably due to the presence of 6% (v/v) DMSO, which lowers the dielectric constant of the medium and therefore promotes electrostatic aggregation.
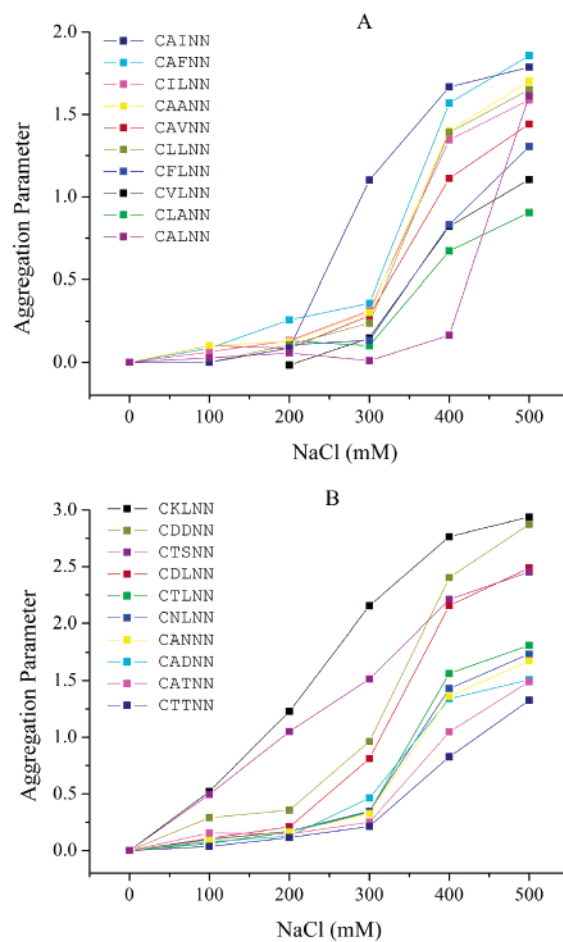
Figure 5. Effect of peptide core on stability of gold nanoparticles. The second and third amino acids were changed into other hydrophobic amino acids (A) or into hydrophilic amino acids (B).

Figure 4B shows the effect of the anchorage group on nanoparticle stability. CALNN and CCALNN possess, respectively, one and two thiols, and a terminal amino group. AALNN
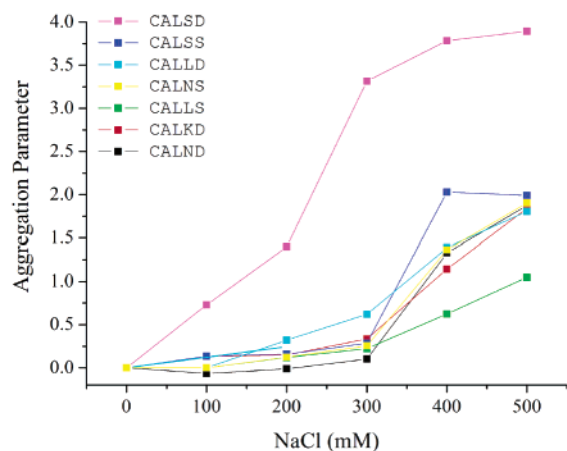
Figure 6. Effect of peptide end (fourth and fifth amino acids) on stability of gold nanoparticles.
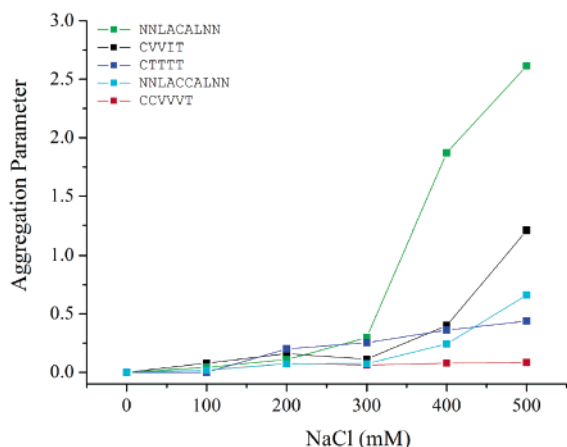
Figure 7. Stability of gold nanoparticles for six peptides designed on different principles.

and KALNN also have the terminal amino group but no thiol; moreover, KALNN possesses a second amino group on the side chain of the N-terminal lysine. Clearly, the thiol group plays a major role in stabilization, since the thiol-containing peptides CALNN and CCALNN show a much greater stability than KALNN and AALNN. Interestingly, aggregation of AALNN-capped nanoparticles occurs at higher concentrations of NaCl than for KALNN-capped nanoparticles. The higher density of terminal amino groups in KALNN may result in a degree of electrostatic repulsion between the peptides, which might prevent the formation of a self-assembled monolayer. Furthermore, hydrophobic interactions due to the additional methyl side chain of alanine in AALNN may also result in an increased stability of AALNN.

Influence of Amino Acids in Positions 2 and 3. The hydrophobic core (second and third amino acids) of the pentapeptide was changed into other hydrophobic amino acids (see Table 1, core, hydrophobic). The nine resulting peptides provided a degree of stabilization of the nanoparticles against NaCl-induced aggregation similar to that of the parental CALNN peptide (Figure 5A). Even bulky aromatic amino acids such as phenylalanine (F) do not seem to disrupt the peptide self-assembled monolayer. Somewhat surprisingly, given that CALNN was designed with a bulkier hydrophobic group at position 3 to take into account particle curvature, bulky hydrophobic side chains (I and F) in position 2 appear to provide better stability

with respect to NaCl-induced aggregation than when present in position 3. Thus, CILNN is more stable than CAINN and CFLNN is more stable than CAFNN.

Charged (K and D) and neutral hydrophilic (T, S, and N) amino acids were substituted into the previously hydrophobic core (Table 1, core, hydrophilic). The presence of charged amino acids results in peptide sequences that generally provide poor protection against aggregation. For example, CDDNN-, CKLNN-, and CDLNN-capped nanoparticles aggregate at low NaCl concentration, although the presence of a negative charge in the third position (CADNN) seems to provide better stability than at the second position (Figure 5B). In contrast, nanoparticles capped with peptides substituted with neutral hydrophilic amino acids, CNLNN, CANNN, CTLNN, CATNN, and CTTNN, generally aggregate at NaCl concentrations comparable to those with peptides possessing hydrophobic cores, although some combinations of neutral hydrophilic amino acids (CTSNN) are not tolerated (Figure 5B).

To summarize the results in Figure 5, the amino acids in positions 2 and 3 appear to require some attractive interaction between neighboring peptide chains to provide stability. Thus, polar and hydrophobic amino acids promote the formation of a self-assembled monolayer through hydrogen bonding and hydrophobic interactions, respectively. However, the electrostatic repulsion of charged amino acids side chains in the core may prevent the formation of a dense peptide layer, hence leading to poor stabilization.

Influence of Amino Acids in Positions 4 and 5. The role of the carboxylic acid terminus of the peptide (Table 1, end) was also addressed. Most of the sequences that were chosen for this study induce immediate aggregation of the nanoparticles upon addition of the peptide. Seven pentapeptide sequences provide a degree of stabilization (Figure 6). Although there is no obvious pattern between stability and the identity of the terminal two amino acids, these results indicate that the charge of the terminal amino acid contributes significantly to the stability of the peptide-capped nanoparticles. Introducing a second terminal negative charge (CALND, CALLD, CALSD, CALKD) reduces the concentration of NaCl that induces aggregation of the peptide-capped nanoparticles (Figure 6). The presence of the extra negative charge, and the absence of H-bonding between terminal amino acids, may affect the peptide packing leading to particles with a surface charge density similar to that of CALNN-capped nanoparticles, but with a less compact protecting peptide layer. H-bonding between the terminal amino acids is likely to play an important role, since replacing the penultimate N with a residue carrying a side chain that is a less amenable to H-bonding, e.g., CALND versus CALSD, reduces the stability.

Design Criteria. The combinatorial analysis globally corroborates the initial design criteria. It establishes the need for a thiol (cysteine) as an anchor to the gold nanoparticle, a clear correlation between peptide length and stability, and the need for cohesive interaction between adjacent peptide chains through hydrophobic interactions or hydrogen bonding to provide high stability. The balance between peptide charge and cohesive interaction is shown to play a major role. The combinatorial analysis also allowed the definition of criteria for peptides leading to the immediate aggregation of the gold nanoparticles.

New Designs. Other sequences, unrelated to CALNN, were also tested. CCVVVT, CVVIT, and CTTTT were chosen for
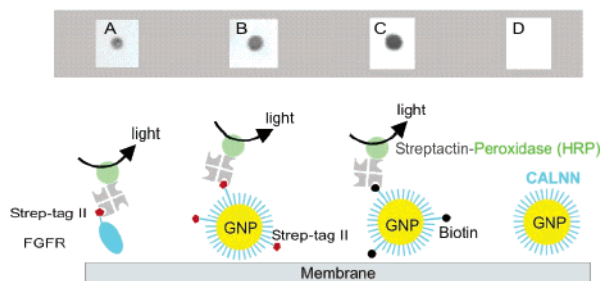
Figure 8. Streptactin peroxidase specific recognition of Strep-tag II and biotin on peptide-capped gold nanoparticles. (A) Engineered fibroblast growth factor receptor (FGFR) with a Strep-tag II sequence. (B) CALNN-capped nanoparticles decorated with Strep-tag II. (C) CALNN-capped nanoparticles decorated with biotin. (D) CALNN-capped nanoparticles.

their strong β-strand forming properties. NNLACALNN and NNLACCALNN possess respectively one and two cysteines in the middle of their sequence. These two peptides should have an overall neutral surface exposed with the carboxylic and amino terminal groups at the peptide−water interface, since it would be expected that bonding will preferentially occur at the central thiol in the cysteine. The presence of the second cysteine (C) greatly improves the stability, maybe by imposing a peptide configuration more favorable to packing. Two of the β-strand forming peptides, CCVVVT and CTTTT, also show very promising behavior, with small values of the aggregation parameter at 500 mM NaCl. In particular, CCVVVT has a greater stability than CALNN with no indication of aggregation at 500 mM NaCl. Considering the relatively small number of sequences tested, the use of larger libraries will allow the identification of capping ligands with even better properties.

Specific Recognition. The introduction of specific recognition groups at the surface of gold nanoparticles is an important prerequisite for their use in bioanalytical assays. In the present case, this is readily achieved by incorporating a proportion of an appropriately functionalized peptide in addition to CALNN in the preparation process. As a proof of principle, we have prepared nanoparticles functionalized with biotin as well as particles modified with a peptide analogue of biotin[46] (Strep-tag II: WSHPQFEK). The conjugates were obtained using a peptide mixture containing on a molar basis 90% CALNN and 10% CALNNGK(biotin)G or CALNNGGWSHPQFEK. The nanoparticles were purified from the excess peptides by size-exclusion chromatography and immobilized on a nitrocellulose membrane. Streptactin peroxidase was then used to detect the presence of biotin and of its peptide analogue on the membrane (Figure 8). A recombinant protein containing Strep-tag II was used as a positive control (Figure 8A) and CALNN-capped nanoparticles as a control for nonspecific interactions. Figure 8 clearly demonstrates the functionalization of the nanoparticles (Figure 8B,C) as well as the absence of nonspecific binding to the CALNN-capped nanoparticles by streptactin peroxidase (Figure 8D).

Summary and Conclusions

Depending on the peptide sequence, addition of peptides to citrate-capped gold nanoparticles can result in the formation of

aggregates or lead to highly stable peptide-capped nanoparticles. Aggregation induced by thiol-containing amino acids has been observed previously and attributed to a cross-linking mechanism sensitive to the detailed peptide structure.[47] Adsorption of lysine followed by a condensation reaction has been used to fabricate an assembly of nanoparticles linked by a dipeptide[48] supporting the interpretation of peptide-induced aggregation as a bridging process due to the presence of multiple sites with strong affinity for gold in different parts of the molecule. When all the gold binding sites are in the same terminus of the peptide, a peptide monolayer forms, leading to peptide-capped nanoparticles.

The stability against NaCl-induced aggregation is strongly dependent on the amino acid sequence. The presence of a thiol and cohesive lateral interactions between the peptides through hydrophobic interactions or hydrogen bonding enhance stability, whereas charged amino acids in the peptide core decrease it. Peptide length correlates with stability similarly to the case of self-assembled monolayers of alkanethiols for which short alkanethiols form more defective films than longer thiols. This is related to hydrophobic interactions leading to better packing of the longer chains.[49,50] It is proposed that the stability of peptide-capped nanoparticles is due to the formation of a compact self-assembled peptide layer. In the case of CALNN, this interpretation is reinforced by the high peptide density at the surface of the nanoparticle. A surface density of 855 ± 70 peptides per nanoparticle corresponding to 1.8 peptides/nm^2 (Materials and Methods) has been measured. Taking into account the volume of one CALNN molecule,[51] this suggests that the peptide is present in an extended configuration (minimum extension is 60% of the fully extended molecule), which is consistent with a parallel β-sheet structure, but not with a close packed α-helical structure.

Above a NaCl concentration threshold, nanoparticles capped with a self-assembled monolayer of peptide aggregate. Interestingly, the spectra are very different from those observed for peptide-induced aggregation. The NaCl-induced and pH-induced aggregation of nanoparticles capped with a self-assembled monolayer provokes a decrease in absorbance at 520 nm and an increase at 650 nm, whereas the peptide-induced aggregation results in a shift of the plasmon peak to a longer wavelength, in an increase in its intensity, and in width broadening (Supporting Information). This observation is compatible with a more densely aggregated structure in the case of peptide-induced aggregation[40] where peptides bridge the nanoparticles, whereas in the NaCl-induced aggregation process, the final distance between particles is governed by the presence of the self-assembled peptide layer (Supporting Information).

In conclusion, a peptide capping ligand has been rationally designed. It has been shown that improved properties and understanding can be gained from a combinatorial approach where the effect of systematic replacement of amino acids on stability is measured. Peptide-capped nanoparticles with properties analogous to a robust protein have been obtained. These nanoparticles are very stable in aqueous buffer; they can be

(46) Skerra, A.; Schmidt, T. G. M. In *Applications of Chimeric Genes and Hybrid Proteins, Part A*; Academic Press: San Diego, London, 2000; Vol. 326, pp 271−304.

(47) Zhang, F. X.; Han, L.; Israel, L. B.; Daras, J. G.; Maye, M. M.; Ly, N. K.; Zhong, C. J. *Analyst* **2002**, *127*, 462−465.
(48) Xu, L.; Guo, Y.; Xie, R.; Zhuang, J.; Yang, W.; Li, T. *Nanotechnology* **2002**, *13*, 725−728.
(49) Bain, C. D.; Troughton, E. B.; Tao, Y. T.; Evall, J.; Whitesides, G. M.; Nuzzo, R. G. *J. Am. Chem. Soc.* **1989**, *111*, 321−335.
(50) Gooding, J. J.; Mearns, F.; Yang, W. R.; Liu, J. Q. *Electroanalysis* **2003**, *15*, 81−96.
(51) Zamyatin, A. A. *Prog. Biophys. Mol. Biol.* **1972**, *24*, 107−123.

freeze-dried, stored as powders, purified by chromatography, and characterized by gel electrophoresis. Importantly, inclusion of a small mole percentage of a longer peptide has no adverse effect on the stability of the peptide-capped nanoparticles. Therefore, it is simple to confer specific molecular recognition properties to the nanoparticles by including a defined percentage of a modified peptide in the preparation process. This approach should enable the development of a library of tags. The versatile properties of peptides as recognition molecules[25,52−54] opens the route to many applications in biology and nanotechnology.

Materials and Methods

Peptides. The peptides CALNN and CALNNGK(biotin)G were purchased from Pepsyn Ltd. (Liverpool, U.K.). Peptide CALNNGG-WSHPQFEK was purchased from Mimotopes Pty Ltd. (Melbourne, Australia). A stock solution of peptide was prepared by dissolving it in phosphate buffer (160 mM NaCl, 3 mM KCl, 8 mM Na_2HPO_4, 1 mM KH_2PO_4). The pH was adjusted to 7.2 using concentrated NaOH, and the resulting 1.9 mM/ml solution was filtered using 0.2 μm filters and kept as aliquots at −80 °C. The peptide was not fully dissolved, and amino acid analysis (Alta Biosciences, Birmingham, U.K.) indicates a final concentration of 1.38 mM after filtering.

Citrate-Coated Gold Nanoparticles. Gold nanoparticles (12.3 nm) were prepared by citrate reduction of $HAuCl_4$.[55−57] An aqueous solution of $HAuCl_4$ (100 mL, 1 mM) was refluxed for 5−10 min, and a warm (50−60 °C) aqueous solution of sodium citrate (10 mL, 38.8 mM) was added quickly. Reflux was continued for another 30 min until a deep-red solution was observed. The solution was filtered through 0.45 μm Millipore syringe filters to remove any precipitate, the pH was adjusted to 7 using dilute NaOH solution, and the filtrate was stored at room temperature.

CALNN-Capped Gold Nanoparticles. If not specified, CALNN-capped gold nanoparticles were prepared by mixing 12.3 nm citrate gold nanoparticles and peptide stock solution in a volume ratio of 10 to 1.

Characterization of Nanoparticle Aggregation by UV−Visible Spectrometry. UV−vis absorption spectra were recorded at room temperature with a Genesys 10-S spectrophotometer (Thermo Spectronics, Rochester, NY). In Figure 3, the CALNN-capped nanoparticles were first separated from free peptide and citrate by size-exclusion chromatography. The pH and NaCl concentration of peptide-capped gold nanoparticles were adjusted and the absorbance spectra were measured after 30 min. For the combinatorial experiment (Figures 4−7), a Spectra Max Plus microplate reader was used (Molecular Devices, Wokingham, U.K.). The aggregation parameter AP is defined as follows: $AP = (A − A_0)/A_0$, where A is the integrated absorbance between 600 and 700 nm and A_0 is the integrated absorbance between 600 and 700 nm of the dispersed solution (neutral pH for Figure 3B and just after peptide addition for Figures 4−7).

Size-Exclusion Chromatography (SEC). Sephadex G25 superfine was purchased from Sigma-Aldrich, Inc., swollen and packed into a glass Econo-Column procured from BioRad Laboratories (Hemel Hemptstead, U.K.). Dilute phosphate-buffered saline was used as the mobile phase (16 mM NaCl, 0.3 mM KCl, 0.8 mM Na_2HPO_4, 0.1 mM KH_2PO_4). All buffers were filtered before use. Flows were gravity driven. Absorbance at 206 nm was recorded in the column effluent using a Uvicord SII single beam UV monitor (Amersham Biosciences Ltd., Bucks, U.K.).

Ion-Exchange Chromatography (IEC). DEAE Sepharose Fast Flow was purchased from BioPharmacia and directly poured in Poly-prep 2 mL plastic columns (BioRad). Fractions (0.2 mL) were collected and the absorbance at 520 nm was measured using the UV−vis spectrophotometer.

Gel Electrophoresis. 1Kb Plus DNA ladder (Invitrogen Ltd., Paisley, U.K.) with ethidium bromide and CALNN-capped nanoparticles were loaded on a 1% (w/v) agarose gel. After migration, DNA was visualized on the gel with UV illumination. Nanoparticles were visible with the unaided eye as a red band (Supporting Information).

Size Distribution and Nanoparticle Concentration. Images of the particles were acquired using a JEOL 2000 EX TEM operating at 200 kV. Specimens for inspection by TEM were prepared by the slow evaporation of one drop of an aqueous solution of the particles placed on a carbon-coated copper mesh grid. IDL 6.0 (Research Systems Inc., Boulder, CO) was used for the determination of the particle size distribution (image processing). A mean diameter of 12.3 nm was obtained with a narrow size distribution (Supporting Information). Using this size distribution and the concentration of gold atoms measured by ICP-AES, the concentration of gold nanoparticle was deduced. This value was then used to calculate the extinction coefficient ϵ ($\epsilon = 0.186 \times 10^9$ mol^{-1} L cm^{-1}).

Number of Peptides per Particle. The number N of CALNN peptides per particle was measured by two independent methods. The first relies on the titration of the peptide using increasing gold nanoparticle concentrations. Six 11 μM CALNN solutions with different concentrations of citrate-stabilized nanoparticles (from 0 to 8 nM) were prepared. After 1 h, the gold nanoparticles were removed by centrifugation and the concentration of remaining free peptide in solution was measured from the absorbance at 196 nm. From a linear fit of the data points (Supporting Information), a ratio of 791 peptides/particle or 1.67 peptides/nm² was found. In the second method, a sample of CALNN-capped nanoparticles was purified from excess peptide using size-exclusion chromatography. The nanoparticle concentration was measured using the absorbance spectrum and the previously determined value of ϵ (see above). The corresponding peptide concentration was obtained from amino acid analysis (Alta Bioscience, Birmingham, U.K.). This second method gave a value of 919 peptides/particle or 1.93 peptides/nm².

Combinatorial. CALNN, CCALNN, amide-terminated CALNN, and NNLAC were bought from Pepsyn Ltd. (Liverpool, U.K.). The other 54 peptides mentioned in Table 1 were bought from Mimotopes Pty Ltd. (Melbourne, Australia). One millimolar peptide solutions in DMSO were prepared, and their effect on nanoparticle stability was studied by adding 13.2 μL of each of these peptide solutions to wells containing 200 μL of citrate-capped gold nanoparticles. After 1 h of reaction, 8 μL of 0.5 M phosphate buffer (pH 7) was added to bring the pH to 7. Then, every 30 min, aliquots of 5 M NaCl pH 7 were added to obtain concentrations of 100, 200, 300, 400, and 500 mM. Before each addition, the absorbance spectrum between 450 and 700 nm was recorded for each well using the microplate reader.

Dot Blot. Samples were deposited onto a nitrocellulose membrane (Amersham Biosciences Ltd., Bucks, U.K.). The membrane was blocked 30 min in a phosphate buffer containing 5 mg/mL bovine serum albumin and then incubated with streptactin peroxidase (IBA, Göttingen, Germany) at a 1:5000 dilution in a phosphate buffer. After five washes, the enzyme activity was revealed using ECL reagents (Amersham Biosciences Ltd., Bucks, U.K.).

(52) Dieckmann, G. R.; Dalton, A. B.; Johnson, P. A.; Razal, J.; Chen, J.; Giordano, G. M.; Munoz, E.; Musselman, I. H.; Baughman, R. H.; Draper, R. K. *J. Am. Chem. Soc.* **2003**, *125*, 1770−1777.
(53) Whaley, S. R.; English, D. S.; Hu, E. L.; Barbara, P. F.; Belcher, A. M. *Nature* **2000**, *405*, 665−668.
(54) Ryadnov, M. G.; Ceyhan, B.; Niemeyer, C. M.; Woolfson, D. N. *J. Am. Chem. Soc.* **2003**, *125*, 9388−9394.
(55) Grabar, K. C.; Freeman, R. G.; Hommer, M. B.; Natan, M. J. *Anal. Chem.* **1995**, *67*, 735−743.
(56) Turkevich, J.; Stevenson, P. C.; Hillier, J. *Discuss. Faraday Soc.* **1951**, 55-&.
(57) Frens, G. *Nature: Phys. Sci.* **1973**, *241*, 20−22.

Supporting Information Available: Effect of freeze-drying and filtering on the absorbance spectra of the CALNN-capped gold nanoparticles. Anion-exchange chromatography of CALNN-capped gold nanoparticles on DEAE-Sepharose. Gel electrophoresis of CALNN-capped nanoparticles. TEM images of CALNN-capped nanoparticles, of aggregated CALNN-capped nanoparticles at pH 1 and of CALSR induced aggregation of gold nanoparticles. Absorbance spectra of peptide-capped nano-

particles in increasing NaCl concentration for the 58 peptides shown in Table 1. Size distribution of the citrate gold nanoparticles and titration of the peptide CALNN using increasing gold nanoparticle concentration to measure the peptide coverage on the nanoparticle surface (PDF). This material is available free of charge via the Internet at http://pubs.acs.org.